

Transition-Metal Borophosphates — Complex Inorganic Frameworks and Magnetism

Bastian Ewald, Walter Schnelle, Ya-Xi Huang, and Rüdiger Kniep

The intensive research on borophosphates started ten years back [1] and revealed a large variety of dense and porous structures [2,3]. The complex anionic partial structures are mainly built of borate and phosphate tetrahedra linked via common oxygen vertices. Thus, like in silicates and aluminosilicates [4], the crystal chemistry of borophosphates comprises a large diversity in structural motifs and dimensionality. As trigonal planar borate groups can also participate in the complex anions, connection patterns similar to those known from borate structures [5,6] can be formed as well.

The presence of transition metal cations is often essential for catalytic [7] and magnetic properties. Synthesis and characterization of borophosphates with magnetically active cations is, thus, one of our main research fields. Furthermore, mixed-valence compounds, low-dimensional magnetic systems and/or quantum-spin systems may be of interest for the research, especially since vanadium-oxides and -phosphates are already part of investigations at our institute [8-10]. Magnetization measurements

yield basic information about magnetically active species and their short and long range interactions. In the following we present three examples of transition-metal borophosphates and their magnetic properties.

The crystal structure of $\text{Rb}_2\text{Co}_3(\text{H}_2\text{O})_2[\text{B}_4\text{P}_6\text{O}_{24}(\text{OH})_2]$ (*Pbca* (Nr. 61), $a = 950(1)$ pm; $b = 1227.2(2)$ pm, $c = 2007.4(2)$ pm, $Z = 4$) comprises a two-dimensionally infinite anionic partial structure of corner-sharing distorted borate and hydrogen phosphate tetrahedra [11]. The layers comprise six- and nine-membered rings of tetrahedra that provide space for the rubidium cations as shown in a cutout in Fig. 1 (top left, Rb^+ omitted).

The crystal structure comprises CoO_6 and $\text{CoO}_4(\text{OH})_2$ coordination octahedra. Each $\text{CoO}_4(\text{H}_2\text{O})_2$ connects on two opposite edges to CoO_6 octahedra, thus, forming isolated trimeric $\text{Co}_3\text{O}_{12}(\text{H}_2\text{O})_2$ units (Fig. 1, bottom left). These interconnect the borophosphate anions which are layerwise arranged with alternating orientation (Fig. 1, right). From the connection via common edges short Co–Co dis-

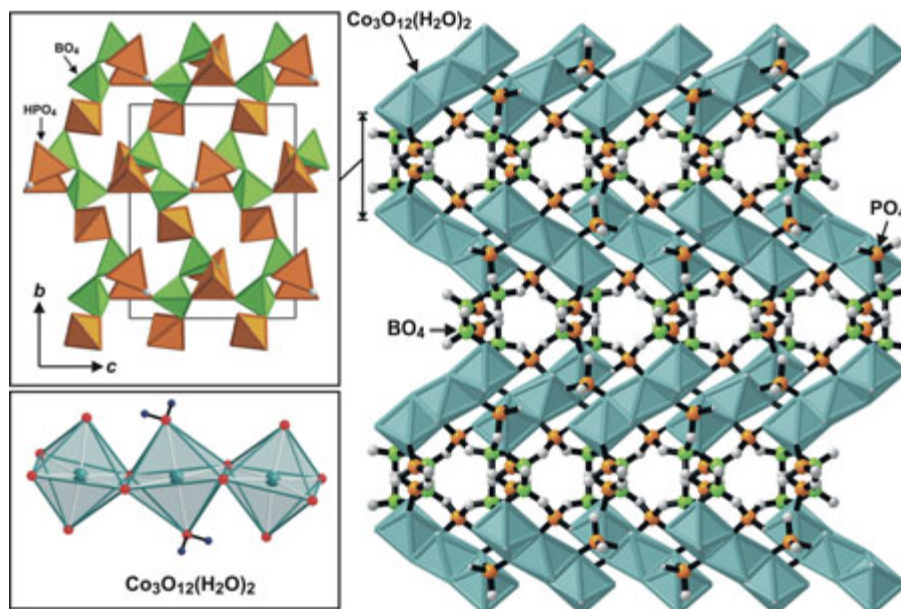


Fig. 1: The crystal structure of $\text{Rb}_2\text{Co}_3(\text{H}_2\text{O})_2[\text{B}_4\text{P}_6\text{O}_{24}(\text{OH})_2]$ contains layers of alternating BO_4^- and HPO_4^- tetrahedra which are connected via common vertices (top left). Trimers of edge-sharing cobalt coordination polyhedra (bottom left) interconnect the borophosphate anions and a layered arrangement results (right). The charge balancing Rb^+ cations are omitted in this illustration.

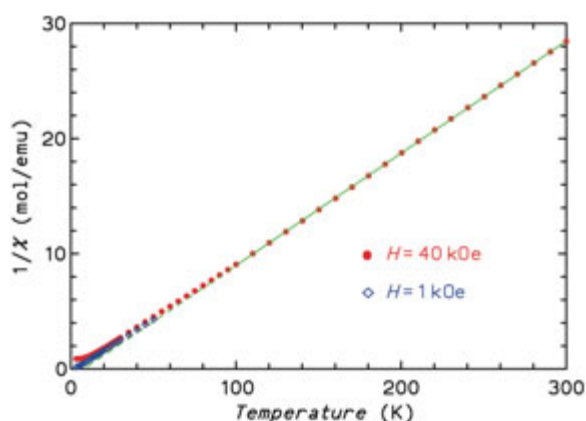


Fig. 2: Inverse molar magnetic susceptibility $1/\chi$ of $\text{Rb}_2\text{Co}_3(\text{H}_2\text{O})_2[\text{B}_4\text{P}_6\text{O}_{24}(\text{OH})_2]$ as a function of temperature in two external fields (green: Curie-Weiss fit).

tances of 333.4(1) pm result. The structural arrangement of $\text{Rb}_2\text{Co}_3(\text{H}_2\text{O})_2[\text{B}_4\text{P}_6\text{O}_{24}(\text{OH})_2]$ is the first example of a structure with trimeric groups of Co^{II} coordination octahedra in the crystal chemistry of borates, phosphates, and borophosphates.

The magnetic susceptibility data ($2 \text{ K} < T < 300 \text{ K}$, H_{ext} from 100 Oe to 70 kOe, Fig. 2) show paramagnetic behavior which can well be described by a Curie-Weiss law at high temperatures (100 K – 300 K). A Weiss-temperature of $\theta = +7.8 \text{ K}$ and an average effective magnetic moment

per Co-atom $\mu_{\text{eff}} = 5.23 \mu_{\text{B}}$ was determined, the latter agreeing with the values observed for octahedrally coordinated Co^{II} cations ($3d^7$ high-spin, $4.7 \mu_{\text{B}} - 5.2 \mu_{\text{B}}$). Although the data below 60 K deviate from the Curie-Weiss fit, no long-range ordering was observed even in a weak field of $H_{\text{ext}} = 100 \text{ Oe}$. The angles $\text{Co}^{\text{II}}-\text{O}-\text{Co}^{\text{II}}$ between adjacent Co^{II} species are $103.35(9)^\circ$ and $98.4(1)^\circ$, respectively. Even though the value of the Weiss-temperature is positive, no signature of this coupling is visible. The product χT increases only little ($< 7\%$) towards lower T while a stronger increase might be expected for ferromagnetic coupling between side species and the central Co position. From our data it seems that the interactions are very small, i.e., the $3d^7$ spin moments behave essentially like single ions.

Interesting magnetic, electrical, and optical properties may result if elements are present in two different oxidation states (mixed valence). Charge transfer between centers with different oxidation state can, e.g., lead to intensive coloring. Furthermore, mixed-valence states have influence on charge carriers in solids as they determine the mobility and, thus, the conductivity. With respect to oxidation states and coordination spheres, the chemistry of vanadium is very flexible and several

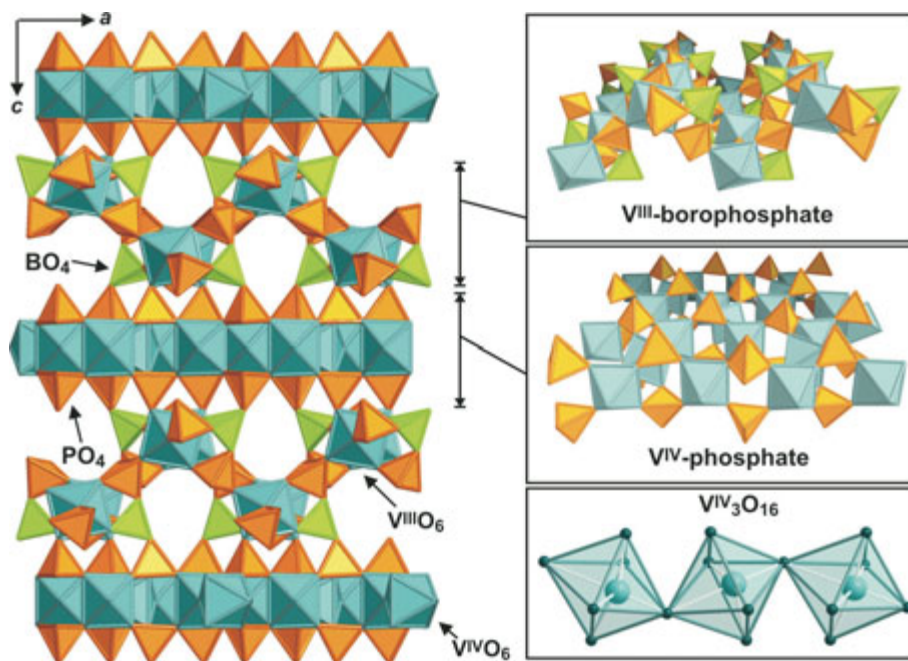


Fig. 3: The inorganic framework of $(\text{C}_3\text{H}_{12}\text{N}_2)(\text{H}_2\text{O})[\text{V}_2^{\text{III}}\text{V}_3^{\text{IV}}\text{B}_2\text{P}_8\text{O}_{30}(\text{OH})_8]$ can be illustrated as a composite of V^{III} -borophosphate- and V^{IV} -phosphate layers (right, top / middle). In the phosphate layers $\text{V}^{\text{IV}}\text{O}_6$ -octahedra are condensed to trimers sharing common vertices (bottom right).

V^{III} -, V^{IV} -, and V^V -borophosphates are known up to date. With the crystal structure of $(C_3H_{12}N_2)_2(H_2O)[V_2^{III}V_3^{IV}B_2P_8O_{30}(OH)_6]$ we now synthesized a first mixed-valence vanadium borophosphate [12]. The inorganic framework of vertex-sharing tetrahedra and octahedra (Fig. 3, left) can be illustrated as a composite of corrugated vanadium(III)-borophosphate layers (Fig. 3, top right) and planar vanadium(IV)-phosphate layers (Fig. 3, middle right). Linked together via common oxygen atoms, these layers are arranged along the c -axis with alternating orientation, and channels parallel to the $[010]$ direction are formed in which the organic cations are located (omitted for clarity). In the phosphate layers a novel connection of distorted $(5+1) V^{IV}O_6$ -octahedra is found: a trimeric unit of three $V^{VI}O_6$ octahedra sharing common vertices (Fig. 3, bottom right).

The magnetic susceptibility can be fitted with the Curie-Weiss law almost over the whole temperature range. An effective magnetic moment $\mu_{\text{eff}} = 5.47 \mu_B$ per f.u. ($\theta = -4.2(1)$ K) was determined. This value is roughly in agreement with the calculated value of $5.00 \mu_B$ per f.u. taking the mixed-valence state with $2 \times V^{III}$ ($2.83 \mu_B$) and $3 \times V^{IV}$ ($1.73 \mu_B$) as refined in the single crystal structure solution. The small value of θ indicates only weak antiferromagnetic exchange interactions. No magnetic ordering is observed above 1.8 K, but $\chi(T)$ increases below 5.0 K in $H_{\text{ext}} = 20$ Oe (no split-

ting of zfc/fc). The isothermal magnetization per f.u. at 1.8 K increases up to $4.12 \mu_B$ at 70 kOe.

The templated iron(III)-borophosphate, $(C_3H_{12}N_2)Fe_6^{III}[B_4P_8O_{32}(OH)_8]$ [12], contains a complex inorganic framework of borophosphate trimers and iron(III) coordination octahedra arranged around channels with ten-membered ring apertures in which the organic diamino-propane cations are located (Fig. 4, left, organic cations omitted for clarity). The crystal structure can be disassembled into iron(III)-borophosphate layers of $FeO_4(OH)(H_2O)$ octahedra interconnecting the borophosphate anions (Fig. 4, top right) which are linked via $FeO_4(OH)_2$ octahedra. Both the different coordination polyhedra around Fe^{III} are shown in Fig. 4 (bottom right).

The inverse magnetic susceptibility of $(C_3H_{12}N_2)Fe_6^{III}[B_4P_8O_{32}(OH)_8]$ versus temperature (Fig. 5) can be described by a Curie-Weiss fit for $T > 50$ K ($H_{\text{ext}} = 1$ kOe). In good agreement with typical values for octahedrally coordinated high-spin Fe^{III} -ions an effective magnetic moment of $\mu_{\text{eff}} = 5.92 \mu_B$ per Fe-atom was obtained. The large Weiss constant of $\theta = -55.4(5)$ K indicates strong antiferromagnetic interactions between the moments. The strong deviations from the Curie-Weiss law observed at low temperatures are shown in the inset of Fig. 5. A spontaneous magnetization is observed which is especially visible in weaker fields. The spontaneous moment is around $0.10 \mu_B$

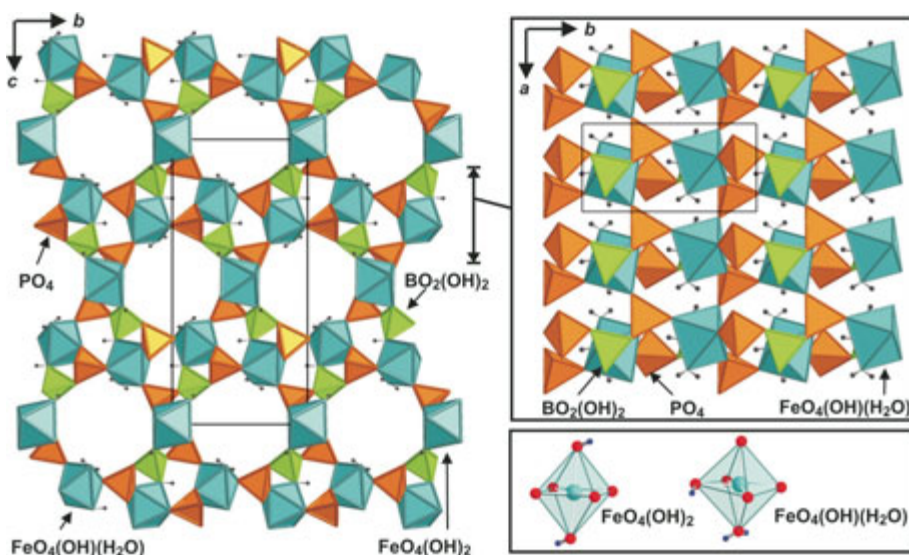


Fig. 4: Complex inorganic framework of borophosphate trimers and iron(III)-coordination octahedra present in the crystal structure of $(C_3H_{12}N_2)Fe_6^{III}[B_4P_8O_{32}(OH)_8]$ (left). The arrangement can be illustrated by iron(III)-borophosphate layers (top right) interconnected by $FeO_4(OH)_2$ octahedra. The two different coordination environments for Fe^{III} are shown in more detail at the bottom right of the figure.

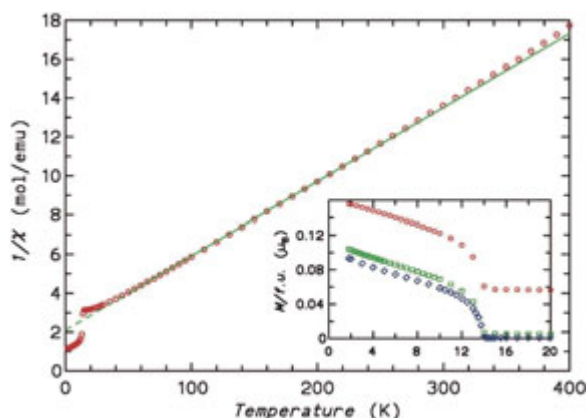


Fig. 5: Inverse magnetic susceptibility of $(C_3H_{12}N_2)Fe_6^{III}[B_4P_8O_{32}(OH)_8]$ for $H_{ext} = 1$ kOe (main plot) and field-cooling magnetization in $H_{ext} = 1$ kOe (red circles), 100 Oe (green squares), and 20 Oe (blue diamonds).

per f.u. Such a low moment is typical for a “weak ferromagnet”. It indicates that a ferromagnetic component exists in a basically antiferromagnetic spin structure of the Fe 3d-moments. It probably originates from spin canting. The ordering is observed at $T_N \approx 14.0(1)$ K.

In conclusion, the featured inorganic framework structures demonstrate the potential of transition metal borophosphates for interesting magnetic systems. Until now the examples are limited to compounds comprising transition metals cations with larger spin numbers (e.g. Mn^{2+} , Fe^{3+}) which have the highest potential for catalysis applications. Borophosphates containing transition metal cations

with low spin numbers (e.g. Cu^{2+}) are promising candidates for novel spin quantum systems (see “*Cu^{II}-Materials — Crystal Chemistry Meets Magnetism*”).

References

- [1] R. Kniep, G. Gözel, B. Eisenmann, C. Röhr, M. Asbrand and M. Kizilyalli, *Angew. Chem.* **106** (1994) 791; *Angew. Chem. Int. Ed. Engl.* **33** (1994) 749.
- [2] R. Kniep, H. Engelhardt and C. Hauf, *Chem. Mater.* **10** (1998) 2930.
- [3] B. Ewald and R. Kniep, in preparation.
- [4] F. Liebau, Springer-Verlag, Berlin, Heidelberg (1985).
- [5] P. C. Burns, J. D. Grice and F. C. Hawthorne, *Canad. Mineral.* **33** (1995) 1131.
- [6] D. Grice, P. C. Burns and F. C. Hawthorne, *Canad. Mineral.* **37** (1999) 731.
- [7] J. B. Moffat, *Cat. Rev. Sci. Eng.* **18** (1978) 199.
- [8] A. A. Gippius, E. N. Morozova, R. V. Spanchenko, E. Kaul, C. Geibel, A. Rabis, M. Baenitz and F. Steglich, *J. Magnetism Magnetic Mater.* **272-276** (2004) 956.
- [9] V. A. Ivanshin, V. Yushankhai, J. Sichelschmidt, D. V. Zakharov, E. E. Kaul and C. Geibel, *J. Magnetism Magnetic Mater.* **272-276** (2004) 960.
- [10] E. E. Kaul, H. Rosner, N. Shannon, R. V. Shpanchenko and C. Geibel, *J. Magnetism Magnetic Mater.* **272-276** (2004) 922.
- [11] H. Engelhardt, W. Schnelle and R. Kniep, *Z. Anorg. Allg. Chem.* **626** (2005) 1380.
- [12] Y.-H. Huang, PhD Thesis, Technical University Dresden, (2005).